

LA-UR-95 1463

Conf-951026--1

Title:

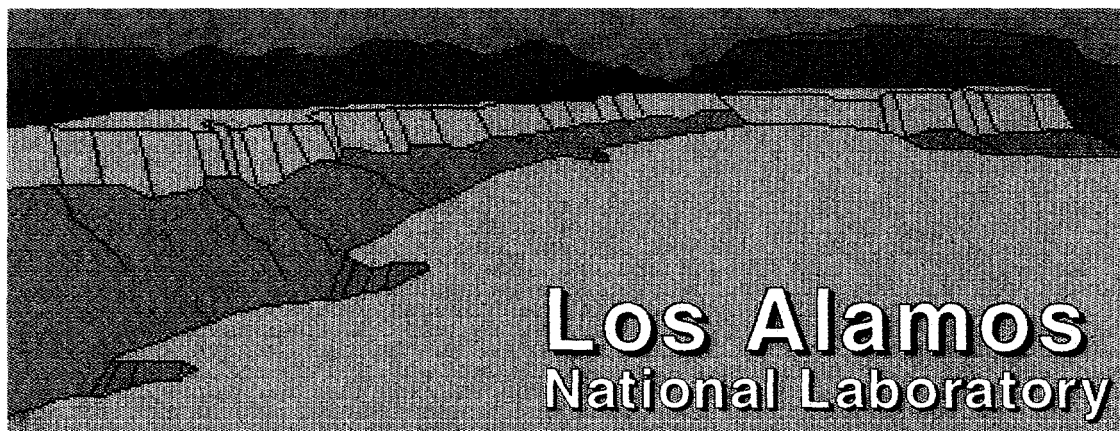
**Characterization of Three Dimensional Fiber Orientation in Short-Fiber Composites**

Author(s):

**Yuntian Zhu  
William R. Blumenthal**

Submitted to:

**TMS/ASM Materials Week 1995,  
Cleveland, OH  
Oct. 29 - Nov. 2, 1995**



Los Alamos National Laboratory, an affirmative action/equal opportunity employer, is operated by the University of California for the U.S. Department of Energy under contract W-7405-ENG-36. By acceptance of this article, the publisher recognizes that the U.S. Government retains a nonexclusive, royalty-free license to publish or reproduce the published form of this contribution, or to allow others to do so, for U.S. Government purposes. The Los Alamos National Laboratory requests that the publisher identify this article as work performed under the auspices of the U.S. Department of Energy. This is a preprint of a paper intended for publication in a journal or proceedings. Because changes may be made before publication, this preprint is made available with the understanding that it will not be cited or reproduced without the permission of the author.

**MASTER**

DISTRIBUTION OF THIS DOCUMENT IS UNLIMITED

et

## **DISCLAIMER**

**Portions of this document may be illegible in electronic image products. Images are produced from the best available original document.**

# **Characterization of Three Dimensional Fiber Orientation in Short-Fiber Composites**

Y. T. Zhu and W. R. Blumenthal  
MST-5, Mail Stop G755  
Materials Science and Technology Division  
Los Alamos National Laboratory  
Los Alamos, NM 87545, USA

## **ABSTRACT**

A mathematical procedure for recovering from image analysis the three dimensional non-symmetric fiber-orientation distribution in short-fiber composites is proposed. Microphotographs from two orthogonal faces of a composite sample are needed to determine the three dimensional fiber orientation. A simple weighting function is derived to take into account the probability of intercepting fibers at varying inclination angles. The present procedure improves the previous works of other researchers in the following two aspects. First, it can obtain the single-angle fiber-orientation distribution from one micrograph in reference to the normal of the photographed surface. This distribution is often needed in predicting the mechanical and physical properties of short-fiber composites in this direction. Second, no symmetry in fiber-orientation distribution is assumed in the determination of the three dimensional fiber-orientation, which makes the present procedure more practical and versatile.

## 1. INTRODUCTION

Short-fiber reinforced composites have the advantages of easy adaptability to conventional manufacturing techniques such as powder metallurgy, casting, molding, drawing, extrusions, machining and welding [1 - 5]. This results in a lower part fabrication cost for short-fiber composites than for long-fiber composites [6]. These advantages have made the short-fiber composites increasingly popular in recent years [7, 8]. With the increasing applications of short-fiber composites comes the need to understand and predict their mechanical and thermal properties, which strongly depend on fiber orientation, length and content [9 - 12]. The fiber orientation is strongly influenced by the flow process during the part fabrication [12, 13]. Short-fibers usually align up in the flow direction to a varying extent so that the intended random fiber orientation is seldom obtained [14]. The non-random fiber orientation leads to anisotropic mechanical and thermal properties of short-fiber composites. In order to assess the composite properties such as strength, Young's modulus and thermal expansion coefficient, it is essential to quantitatively characterize fiber-orientation distribution. [13-15].

Several techniques such as the direct image measurement using an image analyzer [9, 16] and optical diffraction [13, 14] have been attempted to characterize fiber orientation in two or three dimensions. The characterization of fiber orientation in two dimensions is straightforward and has been well studied [14, 15, 17, 18]. However, the characterization of fiber orientation in three dimensions is not as straightforward as it might appear [13]. Microphotographs from two orthogonal faces of a composite sample are needed, and recovering the three dimensional fiber-orientation distribution from the two microphotographs is not trivial, and has not been well studied.

Typically, two different methods are used to describe the three dimensional fiber orientation. One method uses the function  $f(\theta, \phi)$ , where  $\theta$  and  $\phi$  are the in-plane and

out-of-plane angle, respectively [9, 13]. This function enables us to assess the anisotropy of composite properties in any direction. Fischer and Eyerer [9] attempted to characterize the three dimensional fiber orientation using a computer based image analysis. They assumed that a fiber-orientation distribution symmetry exists in the cross-section investigated, which may not be true in most cases. The symmetry exists only when the composite specimen is cut in a few particular orientations, except when the short fibers are perfectly randomly-oriented. They also used a complicated weighting function [9, 11] to correct the inclination-dependent probability of intercepting a fiber by the cross-section investigated.

The other method to characterize the fiber orientation is to use a single angle function  $f(\psi)$ , where  $\psi$  is the angle between a fiber and the direction in which the composite properties is to be assessed (the normal direction of the photographed cross-section). This function is needed to assess the composite properties in the direction normal to the photographed cross-section. Jain and Wetherhold [19] proposed a mathematical procedure to recover  $f(\psi)$  from  $f(\theta, \phi)$ . Gonzalez *et al* [13] proposed another mathematical procedure to recover  $f(\psi)$  from the planar characterization of two orthogonal sections. Both works assumed a symmetry in the fiber-orientation distribution, which makes them not applicable to non-symmetric cases. In addition, there is no need to recover  $f(\psi)$  from  $f(\theta, \phi)$  or perform the planar characterization of two orthogonal sections. As demonstrated later in the present work,  $f(\psi)$  can be obtained directly from the characterization of one planar cross-section.

The objective of this paper is to develop a procedure for obtaining  $f(\psi)$  directly from the characterization of one planar cross-section, and to derive a procedure for recovering the three dimensional non-symmetric fiber-orientation distribution from the micrographs of two planar orthogonal sections.

## 2. SINGLE-ANGLE ORIENTATION FUNCTION $f(\psi)$

The single-angle fiber-orientation distribution function  $f(\psi)$  can be directly obtained from the micrograph of one planar cross-section, where  $0 \leq \psi \leq \pi/2$  is the inclination angle of a fiber toward the normal of the cross-section. The micrograph provides images of fiber cross-section as cut by the planar cross-section. The inclination angle  $\psi$  of each fiber can be obtained from its cross-section image, and the fiber-orientation density  $n(\psi)$ , can be calculated as

$$n(\psi) = n_p(\psi)g(\psi) \quad (1)$$

where  $n_p(\psi)$  is the apparent fiber-orientation density as counted from the planar micrograph and  $g(\psi)$  is a weighting function which is the inverse of the probability of intercepting a fiber with an inclination angle  $\psi$  by the planar cross-section. The single-angle fiber-orientation distribution function  $f(\psi)$  can be calculated by normalizing  $n(\psi)$  :

$$f(\psi) = \frac{n(\psi)}{\int_0^{\pi/2} n(\psi) d\psi} \quad (2)$$

In order to obtain  $n(\psi)$  needed for calculating  $f(\psi)$ , the inclination angle  $\psi$  and the weighting function  $g(\psi)$  have to be obtained first. The procedures for obtaining  $\psi$ ,  $g(\psi)$  and  $n(\psi)$  are described below.

### 2.1 Calculation of the inclination angle $\psi$

When a circular cylindrical fiber is cut by a planar section, an elliptical fiber cross-section is resulted (see Fig. 1). The inclination angle  $\psi$  of the fiber can be calculated as:

$$\psi = \arccos\left(\frac{d}{b}\right) \quad (3)$$

where  $b$  and  $d$  are the major and minor axes of the ellipse, respectively.  $d$  also equals to the fiber diameter. However, if a fiber is cut through its end or if a fiber has an inclination angle  $\psi \approx \pi/2$ , the fiber cross-section will show only a partial ellipse, from which  $d$  and  $b$  may not be able to be measured directly. The possible fiber cross-section shapes are shown in Fig. 2. Using the dimensional data from the partial ellipse as shown in Fig. 2,  $d$  and  $b$  can be calculated from the ellipse equation  $x^2/(d/2)^2 + y^2/(b/2)^2 = 1$ , and  $\psi$  can be subsequently calculated using Eq. 3. The equations as such derived for calculating  $\psi$  for varying fiber cross-section shapes are as follows:

Fig. 2a:

$$\psi = \arccos\left(\frac{\sqrt{e_2^2 - e_1^2/2}}{2c}\right) \quad (4)$$

Fig. 2b:

$$\psi = \arccos\left(\frac{d}{2c}\right) \quad (5)$$

Fig. 2c:

$$\psi = \arccos\left(\frac{\sqrt{2(2e_2^2 - e_1^2 - e_3^2)}}{4c}\right) \quad (6)$$

Fig. 2d:

$$\psi = \arccos\left(\frac{\sqrt{d^2 - e^2}}{2c}\right) \quad (7)$$

Fig. 2e:

$$\psi = \frac{\pi}{2} \quad (8)$$

## 2.2 Derivation of weighting function $g(\psi)$

The probability,  $p(\psi)$ , of a fiber being intercepted by a x-y cutting plane (see Fig. 1) is proportional to  $h+m$ , the projected length of the fiber toward z axis:

$$p(\psi) = K(h+m) \quad (9)$$

where  $K$  is a constant and  $h+m$  can be calculated from the geometry (Fig. 1) as

$$h+m = l \cos \psi + d \sin \psi \quad (10)$$

where  $l$  is the fiber length and  $d$  the fiber diameter. Substituting Eq. 10 into Eq. 9 yields

$$p(\psi) = K(l \cos \psi + d \sin \psi) \quad (11)$$

The weighting function  $g(\psi)$  can be defined as

$$g(\psi) = \frac{p(\psi = \pi/2)}{p(\psi)} = \frac{r}{r \cos \psi + \sin \psi} \quad (12)$$

where  $r = l/d$  is the fiber aspect ratio. This weighting function is much more straightforward and simpler than what was proposed by previous researchers [11]

## 2.3 Calculation of $n(\psi)$

Knowing the fiber inclination angle  $\psi$  and weighting function  $g(\psi)$ , we are ready to calculate fiber-orientation density  $n(\psi)$ . Substituting Eq. 12 into Eq. 1 yields

$$n(\psi) = \frac{r n_p(\psi)}{r \cos \psi + \sin \psi} \quad (13)$$

$n(\psi)$  is usually presented by a histogram [14, 15, 17]. Due to the statistical nature of the fiber-orientation distribution, the histogram is usually rough [14] and difficult to fit by a

smooth function  $n(\psi)$ . In order to overcome this difficulty, we propose to plot the measured accumulative fiber-orientation data

$$N(\psi) = \sum_{i=1}^n \frac{n_p(\psi_i)r}{r \cos \psi_i + \sin \psi_i} \quad \text{for all } \psi_i \leq \psi \quad (14)$$

as a function of  $\psi$ , and then fit the data with a polynomial function:

$$N(\psi) = \sum_{i=0}^k a_i \psi^i \quad (15)$$

where  $n$  is the total number of fibers with an inclination angle  $\psi_i \leq \psi$ ,  $n_p(\psi_i)$  is the number of fibers with an inclination angle  $\psi_i$  as determined from the micrograph, and  $k$  is the highest power in the polynomial function and is fitted for a given regression. By definition,  $n(\psi)$  can be derived from  $N(\psi)$  as

$$n(\psi) = \frac{dN(\psi)}{d\psi} = \sum_{i=1}^k i a_i \psi^{i-1} \quad (16)$$

### 3. Three Dimensional Fiber-orientation Function

Most workers [9, 13, 16, 19] have used the function  $f(\theta, \phi)$  to describe the three dimensional fiber-orientation distribution. We adopt here the function  $f(\theta, \psi)$  [18] instead of  $f(\theta, \phi)$  for mathematical simplicity in its derivation and application. There is no substantial difference between these two functions since  $\psi$  and  $\phi$  are related as  $\psi + \phi = \pi/2$  (see Fig. 3). As did other workers[13, 19], we assume that  $f(\theta, \psi)$  can be expressed as

$$f(\theta, \psi) = f(\theta)f(\psi) \quad (17)$$

with a normalizing condition as

$$\iint_{\substack{0 \leq \theta < 2\pi \\ 0 \leq \psi < \pi/2}} f(\theta, \psi) d\theta d\psi = \int_0^{2\pi} f(\theta) d\theta \int_0^{\pi/2} f(\psi) d\psi = 1 \quad (18)$$

where  $f(\psi)$  is already calculated by Eq. 2. With  $f(\psi)$  known, the task of obtaining  $f(\theta, \psi)$  is reduced to obtaining  $f(\theta)$ . Since  $f(\psi)$  is already normalized (Eq. 2), the normalizing condition in Eq. 18 can be reduced to:

$$\int_0^{2\pi} f(\theta) d\theta = 1 \quad (19)$$

However, it is not straight forward to determine  $f(\theta)$  without assuming any symmetry for the fiber-orientation distribution. It can be seen from Fig. 4 that the shapes and orientations of the fiber cross-sections do not differentiate a fiber with an orientation  $(\theta, \psi)$  from a fiber with an orientation  $(\theta + \pi, \psi)$ . Therefore,  $f(\theta)$  can not be determined from the micrograph of one cross-section of a composite sample, and at least two micrographs from two orthogonal cross-sections are needed. What can be obtained from the micrograph of one cross-section (say the cross-section perpendicular to the z axis in Fig. 3) is

$$\tilde{f}(\theta) = f(\theta) + f(\theta + \pi) \quad 0 \leq \theta < \pi \quad (20)$$

where  $\tilde{f}(\theta)$  is the apparent fiber-orientation distribution as a function of  $\theta$  and can be determined from the planar micrograph in the same way as  $f(\psi)$  is determined:

$$\tilde{f}(\theta) = \frac{\tilde{n}(\theta)}{\int_0^{\pi} \tilde{n}(\theta) d\theta} \quad (21)$$

where  $\tilde{n}(\theta)$  is the apparent fiber-orientation density distribution as a function of  $\theta$  and can be determined in the following way. First plot the measured accumulative fiber-orientation data

$$\tilde{N}(\theta) = \sum_{i=1}^n \tilde{n}(\theta_i) \quad \text{for all } \theta_i \leq \theta \quad (22)$$

as a function of  $\theta$ , and then fit the data with a polynomial function:

$$\tilde{N}(\theta) = \sum_{i=0}^m b_i \theta^i \quad (23)$$

where  $n$  is the total number of fibers with an inclination angle  $\theta_i \leq \theta$ ,  $\tilde{n}(\theta_i)$  is the number of fibers with an orientation  $\theta_i$ , and  $m$  is the highest power in the polynomial function and is determined during the curve fitting. By definition,  $\tilde{n}(\theta)$  can be derived from  $\tilde{N}(\theta)$  as

$$\tilde{n}(\theta) = \frac{d\tilde{N}(\theta)}{d\theta} = \sum_{i=1}^m i b_i \theta^{i-1} \quad (24)$$

Substituting Eq. 24 into Eq. 21 yields

$$\tilde{f}(\theta) = \frac{\sum_{i=1}^m i b_i \theta^{i-1}}{\sum_{i=1}^m b_i \pi^i} \quad (25)$$

It can be seen that  $\tilde{f}(\theta)$  is a (m-1)th order polynomial.

Let us assume that  $\tilde{f}(\theta)$  in Eq. 25 is obtained from the specimen cross-section perpendicular to z axis. Another set of fiber-orientation functions,  $f_y(\psi_y)$  and  $\tilde{f}_y(\theta_y)$  (see Fig. 3 for the definition of  $\psi_y$  and  $\theta_y$ ), can be obtained in the same way as  $f(\psi)$  and  $\tilde{f}(\theta)$  are obtained. The two sets of fiber-orientation functions obtained from these two orthogonal cross-sections contain enough information for determining  $f(\theta)$ . Assume that  $\tilde{f}_y(\theta_y)$  takes a similar form to  $\tilde{f}(\theta)$ :

$$\tilde{f}_y(\theta_y) = \frac{\sum_{i=1}^j ic_i \theta_y^{i-1}}{\sum_{i=1}^j c_i \pi^i} \quad (26)$$

Then,  $\tilde{f}_y(\theta_y)$  is a (j-1)th order polynomial. Similar to Eq. 20, we also have

$$\tilde{f}_y(\theta_y) = f_y(\theta_y) + f_y(\theta_y + \pi) \quad 0 \leq \theta_y < \pi \quad (27)$$

The next step is to derive  $f(\theta)$  from the above two sets of functions obtained from the experimental measurements. Let us assume that  $f(\theta)$  takes the form of a (m+j-2)th order polynomial:

$$f(\theta) = \sum_{k=0}^{j+m-2} u_k \theta^k \quad (28)$$

Substituting Eq. 28 into Eq. 20 yields

$$\tilde{f}(\theta) = \sum_{k=0}^{j+m-2} u_k [\theta^k + (\theta + \pi)^k] \quad 0 \leq \theta < \pi \quad (29)$$

In order to utilize  $f_y(\psi_y)$  and  $\tilde{f}_y(\theta_y)$  in the determination of  $f(\theta)$ , the relationship between  $\tilde{f}_y(\theta_y)$  and  $f(\psi)$ ,  $f(\theta)$  has to be first derived. This can be done by expressing  $f_y(\theta_y)$  and  $f_y(\theta_y + \pi)$  in terms of  $f(\psi)$  and  $f(\theta)$  using the Leibniz rule for the differentiation of integrals [20]. We have to first find the equivalent domains of integration. It can be seen from Fig. 5 that an integration domain  $\theta_y \in (0, \theta_y)$  and  $\psi_y \in (0, \psi_y)$  for  $f_y(\theta_y)$  and  $f_y(\psi_y)$ , where  $\theta_y \leq \pi/2$ , is equivalent to  $\theta \in (\theta_1, \theta_2)$  and  $\psi \in (\psi_1, \pi/2)$  for  $f(\psi)$  and  $f(\theta)$ . It can also be seen from Fig. 5 that  $\theta_1$  is a function of  $\psi$  and  $\psi_y$ ,  $\theta_2$  is a function of  $\psi$  and  $\theta_y$  and  $\psi_1$  is a function of  $\theta_y$  and  $\psi$ .  $\theta_1$ ,  $\theta_2$  and  $\psi_1$  can be found with a little geometry from Fig. 3:

$$\theta_1 = \arcsin\left(\frac{\cos \psi_y}{\sin \psi}\right) \quad (30a)$$

$$\theta_2 = \arccos(\cot \theta_y \cot \psi) \quad (30b)$$

and

$$\psi_1 = \arccos(\sin \psi_y \sin \theta_y) \quad (30c)$$

The accumulative fiber-orientation function,  $F$ , in terms of  $f_y(\psi_y)$  and  $f_y(\theta_y)$  within the above integration domain is

$$F = \int_0^{\psi_y} f_y(\psi_y) d\psi_y \int_0^{\theta_y} f_y(\theta_y) d\theta_y \quad (31)$$

$F$  can also be expressed in terms of  $f(\psi)$  and  $f(\theta)$  in the same integration domain as

$$F = \int_{\psi_1}^{\pi/2} f(\psi) d\psi \int_{\theta_1}^{\theta_2} f(\theta) d\theta \quad (32)$$

Eq. 31 is equivalent to Eq. 32, which yields

$$\int_0^{\psi_y} f_y(\psi_y) d\psi_y \int_0^{\theta_y} f_y(\theta_y) d\theta_y = \int_{\psi_1}^{\pi/2} f(\psi) d\psi \int_{\theta_1}^{\theta_2} f(\theta) d\theta \quad (33)$$

Substituting Eq. 28 into Eq. 33, integrating  $f(\theta)$  and rearranging yield

$$\int_0^{\theta_y} f(\theta_y) d\theta_y = \frac{1}{\int_0^{\psi_y} f(\psi_y) d\psi_y} \sum_{k=0}^{j+m-2} \frac{u_k}{k+1} \int_{\psi_1}^{\pi/2} f(\psi) (\theta_2^{k+1} - \theta_1^{k+1}) d\psi \quad (34)$$

Substituting Eqs. 30a and 30b into Eq. 34 and differentiating it yields

$$f_y(\theta_y) = \frac{1}{\int_0^{\psi_y} f_y(\psi_y) d\psi_y} \sum_{k=0}^{j+m-2} u_k \int_{\psi_1}^{\pi/2} \frac{f(\psi) \arccos^k(\cot \theta_y \cot \psi)}{\sin^2 \theta_y \sqrt{\tan^2 \psi - \cot^2 \theta_y}} d\psi \quad (35)$$

In the next step, we need to express  $f(\psi_y)$  and  $f(\theta_y + \pi)$  in terms of  $f(\psi)$  and  $f(\theta)$ . Fiber  $a$  in Fig. 3 has an orientation  $(\theta_y, \psi_y)$  or  $(\theta, \psi)$ . Let us rotate fiber  $a$  into fiber  $b$  orientation which is  $(\theta_y + \pi, \psi_y)$ . Fiber  $b$  is equivalent to fiber  $c$  which has an orientation  $(2\pi - \theta, \psi)$ , that is, the fiber orientation  $(\theta_y + \pi, \psi_y)$  is equivalent to orientation  $(2\pi - \theta, \psi)$ . Following this logic, one can easily figure out that an integration domain  $\theta_y \in (\pi, \theta_y + \pi)$  and  $\psi_y \in (0, \psi_y)$  for  $f_y(\theta_y)$  and  $f_y(\psi_y)$ , where  $\theta_y \leq \pi/2$ , is equivalent to  $\theta \in (2\pi - \theta_2, 2\pi - \theta_1)$  and  $\psi \in (\psi_1, \pi/2)$  for  $f(\psi)$  and  $f(\theta)$ . For this new integration domain (represented in shadow on the left part of Fig. 5), an equation similar to Eq. 33 can be obtained

$$\int_0^{\psi_y} f_y(\psi_y) d\psi_y \int_{\pi}^{\theta_y + \pi} f_y(\theta_y) d\theta_y = \int_{\psi_1}^{\pi/2} f(\psi) d\psi \int_{2\pi - \theta_2}^{2\pi - \theta_1} f(\theta) d\theta \quad (36)$$

and the following equation can be derived in the same way as Eq. 35 was:

$$f_y(\theta_y + \pi) = \frac{1}{\int_0^{\psi_y} f_y(\psi_y) d\psi_y} \sum_{k=0}^{j+m-2} u_k \int_{\psi_1}^{\pi/2} \frac{f(\psi) [2\pi - \arccos(\cot \theta_y \cot \psi)]^k}{\sin^2 \theta_y \sqrt{\tan^2 \psi - \cot^2 \theta_y}} d\psi \quad (37)$$

Substituting Eqs. 35 and 37 into Eq. 27 and rearranging yields

$$\begin{aligned} \tilde{f}_y(\theta_y) \int_0^{\psi_y} f_y(\psi_y) d\psi_y = \\ \sum_{k=0}^{j+m-2} u_k \int_{\psi_1}^{\pi/2} f(\psi) \frac{\arccos^k(\cot \theta_y \cot \psi) + [2\pi - \arccos(\cot \theta_y \cot \psi)]^k}{\sin^2 \theta_y \sqrt{\tan^2 \psi - \cot^2 \theta_y}} d\psi \end{aligned} \quad (38)$$

where  $0 \leq \theta_y < \pi/2$ .

It can be seen from Eq. 28 that there are  $j+m-1$  coefficients ( $u_0$  to  $u_{j+m-2}$ ) to be determined in order to determine the polynomial  $f(\theta)$ . Taking  $m$   $\theta$  values ( $0 \leq \theta < \pi$ ) and substituting them into Eq. 29, we can obtain a group of  $m$  linear equations. In the same way, we can obtain another group of  $j-1$  linear equations by substituting  $j-1$   $\theta_y$  and

$\psi_y$  values ( $0 \leq \theta_y < \pi/2$ ,  $0 \leq \psi_y < \pi/2$ ) into Eq. 38. The  $j+m-1$  coefficients, and therefore  $f(\theta)$ , can be easily obtained by solving the total number of  $j+m-1$  linear equations. The three dimensional fiber-orientation function  $f(\theta, \psi)$  can be subsequently obtained by substituting the  $f(\theta)$  and  $f(\psi)$  into Eq. 17.

### Conclusions

The three dimensional short-fiber-orientation distribution in a real composite usually does not have any symmetry. The works by previous researchers assume a symmetry in characterizing the fiber-orientation distribution in three dimensions, which is idealistic. The present procedure improves the works by previous researchers by not assuming any symmetry, and can be used to characterize the *non-symmetric* three-dimensional fiber orientation. The present work also derives a simple fiber-orientation weighting function and equations to calculate the fiber inclination angle for different fiber cross-sections. A procedure was developed to obtain the single angle fiber-orientation distribution function from one micrograph, which can avoid the unnecessary tedious calculation of it from the three dimensional fiber orientation or from micrographs of two orthogonal composite cross-sections.

### References

1. P. E. Chen, *Polymer Engineering and Science* **11**, 51 (1971).
2. P. K. Liaw, J. G. Gregg and W. A. Logsdon, *J. Material Science* **22**, 1613 (1987).
3. S. K. Gaggar and L. J. Broutman, *Polymer Engineering and Science* **16**, 537 (1976).

4. L. A. Goetler, *Concise Encyclopedia of Composite Materials*, Revised Edition, A. Kelly, Ed., Elsevier Science Ltd., Oxford, England, p. 90 (1994).
5. J. V. Milewski, *Concise Encyclopedia of Composite Materials*, Revised Edition, A. Kelly, Ed., Elsevier Science Ltd., Oxford, England, p. 313 (1994).
6. Y. Takao, *Recent Advances in composites in the United States and Japan*, ASTM STP 864, J. R. Vinson and M. Taya, Eds., American Society for Testing and Materials, Philadelphia, pp. 685-699 (1985).
7. C. M. Friend, *J. Materials Science* **22**, 3005 (1987).
8. Y. T. Zhu, G. Zong, A. Manthiram and Z. Eliezer, *J. Materials Science* **29**, 6281 (1994).
9. G. Fischer and P. Eyerer, *Polymer Composites* **9**, 297 (1988).
10. S. R. Doshi, J. M. Dealy and J. -M. Charrier, *Polymer Engineering and Science* **26**, 468 (1986).
11. B. Moginger and P. Eyerer, *Composites* **22**, 394 (1991).
12. R. B. Pipes, R. L. McCullough and D. G. Taggart, *Polymer Composites* **3**, 34 (1982).
13. L. M. Gonzalez, F. L. Cumbreira, F. Sanchez-Bajo and A. Pajares, *Acta Metallurgica et Materialia* **42**, 689 (1994).
14. S. H. McGee and R. L. McCullough, *J. Applied Physics* **55**, 1394 (1984).
15. R. C. Wetherhold and P. D. Scott, *Composites Science and Technology* **37**, 393 (1990).
16. S. W. Yurgartis, *Composites Science and Technology* **30**, 279 (1987).
17. M. Vincent and J. F. Agassant, *Polymer Composites* **7**, 76 (1986).
18. H. T. Kau, *Polymer Composites* **8**, 82 (1987).
19. L. K. Jain and R. C. Wetherhold, *Acta Metallurgica et Materialia* **40**, 1135 (1992).
20. M. L. Boas, *Mathematical Methods in the Physical Science*, p. 162, Wiley, New York (1966).

## Captions

- Fig. 1. A fiber with an inclination angle  $\psi$  toward  $z$  axis is cut by  $x$ - $y$  plane, which results in an elliptical fiber cross-section.
- Fig. 2. All possible cross-section shapes when a fiber end is cut.
- Fig. 3. Definitions of  $\theta$ ,  $\psi$ ,  $\theta_y$  and  $\psi_y$ . Fiber  $b$  is equivalent to fiber  $a$  being rotated around  $y$  axis by  $\pi$  degree and fiber  $c$  is equivalent to fiber  $b$  in orientation.
- Fig. 4. Two fibers with the same inclination angle  $\psi$  and  $\Delta\theta = \pi$  can not be differentiated by the cross-section cut by  $x$ - $y$  plane.
- Fig. 5. The integration domain for Eqs. 31 through 38.

## DISCLAIMER

This report was prepared as an account of work sponsored by an agency of the United States Government. Neither the United States Government nor any agency thereof, nor any of their employees, makes any warranty, express or implied, or assumes any legal liability or responsibility for the accuracy, completeness, or usefulness of any information, apparatus, product, or process disclosed, or represents that its use would not infringe privately owned rights. Reference herein to any specific commercial product, process, or service by trade name, trademark, manufacturer, or otherwise does not necessarily constitute or imply its endorsement, recommendation, or favoring by the United States Government or any agency thereof. The views and opinions of authors expressed herein do not necessarily state or reflect those of the United States Government or any agency thereof.

---

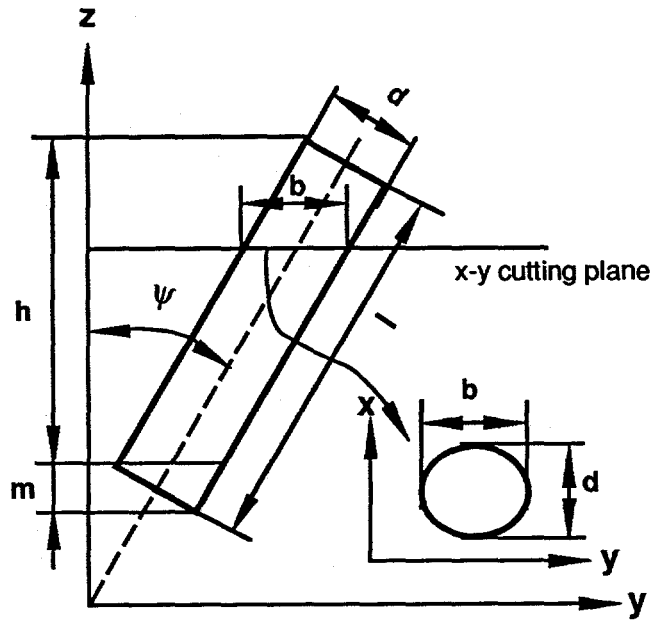
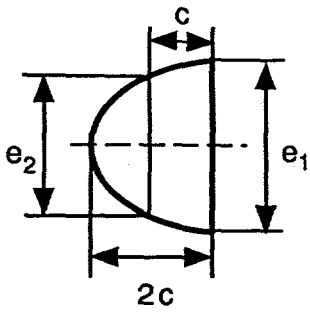
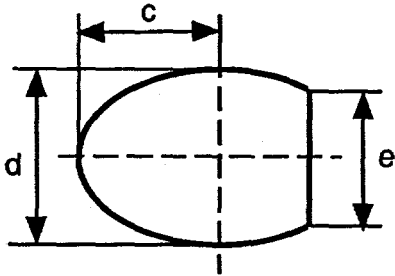


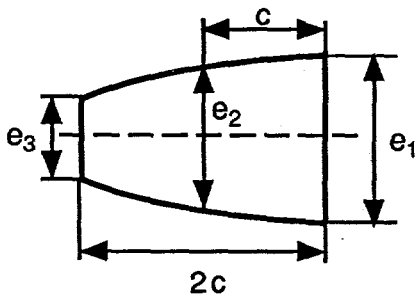
Fig.1



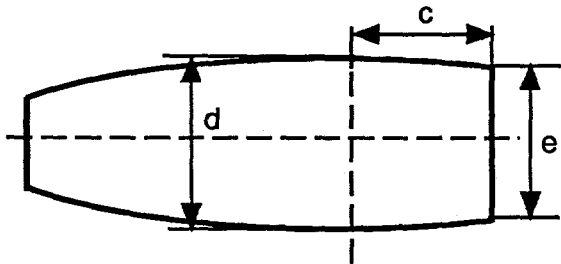
(a)



(b)



(c)



(d)



(e)

Fig. 2

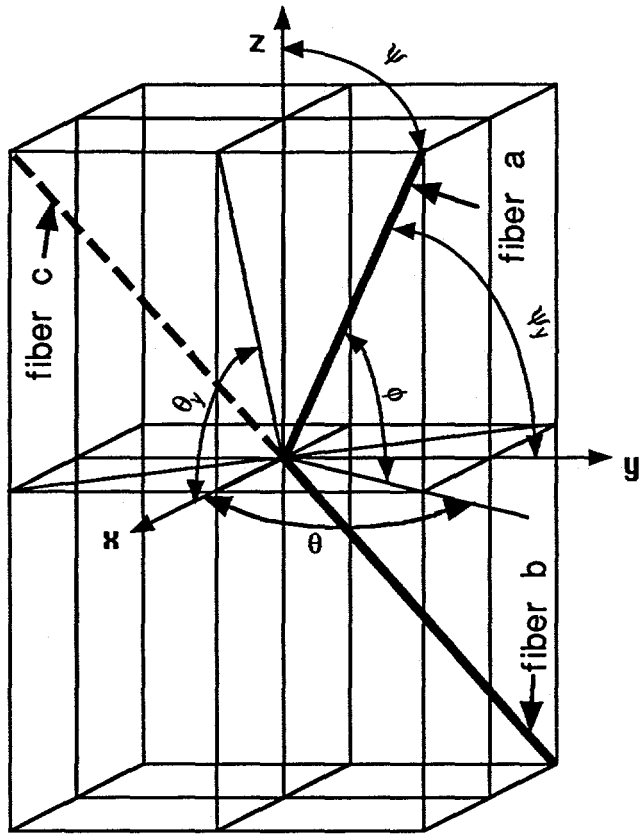


Fig. 3

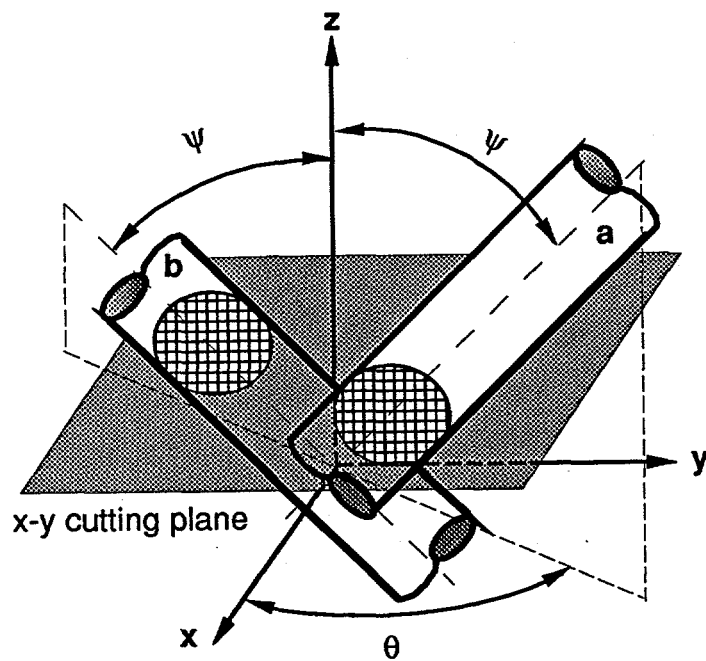


Fig. 4

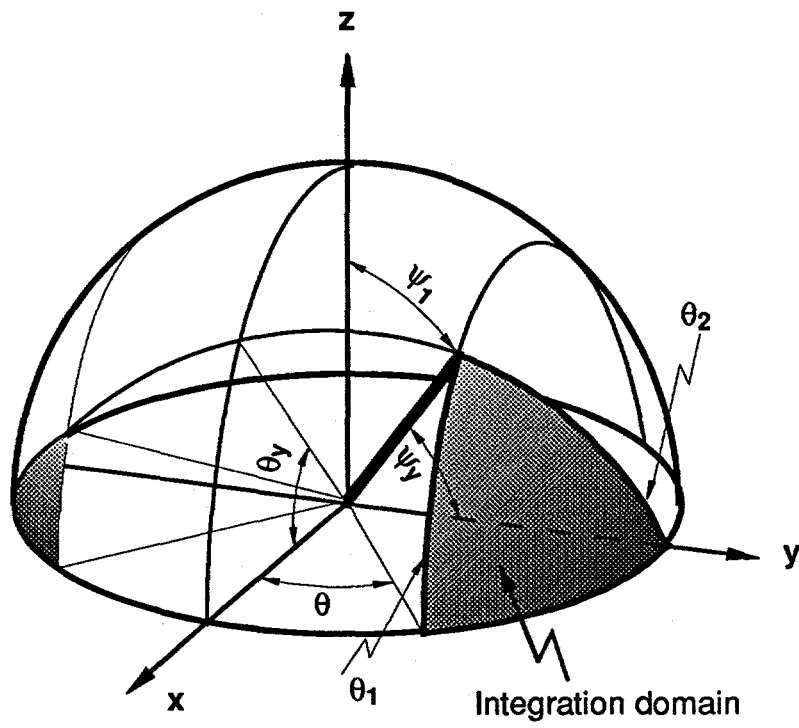


Fig. 5.